Symposium on Thermoacoustics in Combustion: Industry meets Academia (SoTiC 2025)
Sept. 8 - Sept. 11, 2025
Trondheim, Norway
Paper No.: 24

Impact of Flame Thickening on the Predicted Shape and Dynamics of a Turbulent Premixed Flame

Cillian Thomas[1] , Alex M. Garcia[2], Stephen Spence[1], Charles Stuart[1], Marc Furi[3], Sandeep Jella[3], Gilles Bourque[4]

Abstract

This study investigates the impact of flame thickening on the predicted flame shape and transfer function of a premixed methane–air turbulent flame using Large Eddy Simulations (LES). Simple 1D flames were used to identify the general impact of thickening on premixed methane-air flames, followed by a 3D LES study to demonstrate the implications of these effects. The flame was shown to increase in length, with a more broad distribution of heat release rate, as thickening factor increased due to changes in flame consumption speed and its response to strain. The Flame Transfer Function (FTF) was computed for each case, and the differences are discussed. It is shown clearly that the thickening factor F can suppress the appearance of vortex shedding modes by increasing the cut-off frequency of the flame. It has also been shown that decreasing thickening factor can cause the appearance of peaks in the FTF which are not observed experimentally. In this study, large thickening factors were shown to cause the flame to leave the combustor domain and lack the ability to conserve energy. This paper highlights clearly the impact of thickening factor on the flame transfer function and the impulse response.

Keywords

Flame Transfer Function, Large Eddy Simulation, Artificially Thickened Flame, Premixed Flame

Introduction

Thermoacoustic instabilities present a significant design and operational challenge in the development of advanced gas turbines capable of operating with low emissions and alternative fuels like hydrogen. Numerical tools such as Large Eddy Simulation (LES) are often used to aid in the prediction and mitigation of these instabilities while keeping the cost of experimental testing to a minimum. A common approach is to predict the Flame Transfer Function (FTF) via LES, and use the FTF in a low order acoustic solver to predict the growth rate and frequency of unstable modes[1]. The growth rates of the predicted modes are particularly sensitive to the FTF, and hence accurate prediction of the FTF is paramount for reliable prediction of thermoacoustic instabilities. The FTF is defined as:

$$\mathcal{F}(\omega) = \frac{\dot{q}'/\bar{\dot{q}}}{u'/\bar{u}} \qquad (1)$$

where $x', \overline{x}$ represent fluctuating and mean quantities respectively, $\bar{\dot{q}}$ is the mean heat release rate, $\bar{u}$ is the mean velocity at a reference location, and ω is frequency.

Accurate prediction of the FTF via LES relies on a combustion model that can accurately represent the heat release rate distribution, and the response of the flame to velocity fluctuations. The Artifically Thickened Flame (ATF) model has been used in many studies to successfully predict thermoacoustic modes[2–4] and the flame response[5–7]. Kuhlmann et al.[8] compared the ATF against the Flame Surface Density (FSD) model for computing the FTF, and concluded that the ATF model required less computational time than the FSD model and less constants or sub models needed to be adjusted. This makes the ATF model a very attractive approach for prediction of the FTF. Despite the relative success of the models, recent studies have highlighted issues associated with the effect of flame thickening on the response to stretch.

Using a 1D counterflow premixed flame, Popp et al.[9] showed that thickening a stretched flame changes the gradients across the flame front and increases the effective stretch level experienced by the flame, leading to $\kappa_{eff} = F\kappa$. For lean methane air flames, this leads to an under prediction of consumption speed. Various authors have proposed methodologies to tackle this issue, including modifying species transport properties and extending the thickened flame model[9–12].

Due to the known impact of the thickening factor on the consumption speed of flame, the aim of this study is to explore LES predictions of a turbulent premixed CH_4-air flame with varying thickening factors, and to focus on how this affects the flame dynamics via the FTF. To the authors' knowledge, this has not been detailed in the literature. This

[1]Department of Mechanical, Manufacturing & Biomedical Engineering, Trinity College Dublin, Dublin, Ireland
[2]Department of Engineering Physics and Computation, TUM School of Engineering and Design, Technical University of Munich, Garching, Germany
[3]Siemens Energy Canada, Montreal, Canada
[4] Alternative Fuels Laboratory, McGill University, Montreal, Canada

Corresponding author:
Cillian Thomas
Email: thomasci@tcd.ie

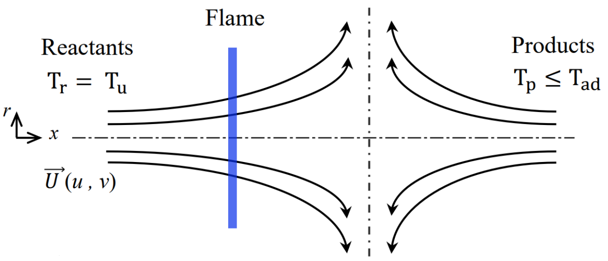

Figure 1. 1D reactant to product flame [14]

will be done by first introducing the impact of thickening for a 1D flame. The analysis will then be extended to explore the impact of F in an LES case. Finally, the FTF will be computed to show the impact on the flame response.

1D Reactant to Product Flames

Impact of Thickening on Consumption Speed

Firstly, the impact of thickening on stretched flames is introduced for a 1D flame. This is done by analyzing a generalised reactant to product (RTP) counterflow flame, as shown in Figure 1, which allows the analysis of a flame at varying levels of stretch. This can be done using Cantera software [13] (more details of this configuration have been presented by Garcia et al. [14]).

The governing equation the mass fraction of a chemical species Y_k is given by:

$$\rho u \frac{\mathrm{d}\,Y_k}{\mathrm{dx}} = \frac{\mathrm{d}}{\mathrm{dx}}\left(\rho D \frac{\mathrm{d}\,Y_k}{\mathrm{dx}}\right) + \dot{\omega}_k \tag{2}$$

where ρ is the density, u is the velocity, D is the mass diffusivity, and $\dot{\omega}_k$ is the reaction rate of species Y_k. Applying thickening to this flame results in the equation for chemical species being given by:

$$\rho u \frac{\mathrm{d}\,Y_k}{\mathrm{dx}} = \frac{\mathrm{d}}{\mathrm{dx}}\left(\rho F D \frac{\mathrm{d}\,Y_k}{\mathrm{dx}}\right) + \frac{\dot{\omega}_k}{F} \tag{3}$$

This increases the flame thickness by a factor F by increasing the diffusivity of the flame, but conserves the laminar flame speed by division of the reaction rate term by F also. The benefit of this model is it allows computation of flames on much coarser grids, which reduces computational cost. The base version of Cantera does not include this modification to allow for flame thickening, hence a custom version of Cantera is used in this study which has been developed by CERFACS [15].

For unstretched 1D flames (i.e freely propagating flames) which propagate at the laminar flame speed, the propagation speed of thickened flames is unchanged, but when the flame is stretched in a stagnation flow, Popp et. al. showed that the convective term is changed by a factor of 1/F [9]. This results in the flame experiencing a stretch level $\kappa_{eff} = \kappa \times F$ compared to the applied stretch κ. To analyse this effect, the consumption speed of the 1D RTP flame was analysed at various thickening factors, where consumption speed is defined here as [14]:

$$S_{c,\dot{q}} = \frac{1}{\rho_u \Delta H_c^0 (Y_{f,b} - Y_{f,u})} \int_{-\infty}^{\infty} \dot{q}\, dx \tag{4}$$

where ρ_u is the unburned density, ΔH_c^0 is the lower heating value of the fuel, $Y_{f,b}$ is the mass fraction of fuel in the burned gases, and simularly $Y_{f,u}$ is the mass fraction of fuel in the unburned gases, $\dot{q}$ is heat release rate, and x indicates axial direction (see Figure 1).

A lean ($\phi = 0.7$) methane-air flame was simulated using the detailed C3MechLite mechanism, containing 61 species and 539 reactions. This mechanism is derived from detailed experimental and numerical data from the C3MechCore kinetic model [16], a detailed mechanism which consists of rigorous experimental and numerical validation. Thickening factors of $F = 1, 3, 6, 8$ were tested with stretch levels $\kappa = 0 - 8,000$ (1/s), and the resulting consumption speed is shown in Figure 2a where it can be seen that the consumption speed of a thickened flame drops rapidly due to F. It is also shown in Figure 2b, that when the consumption speed is plotted against $\kappa \times F$, the curves collapse onto one, demonstrating this effective stretch phenomenon.

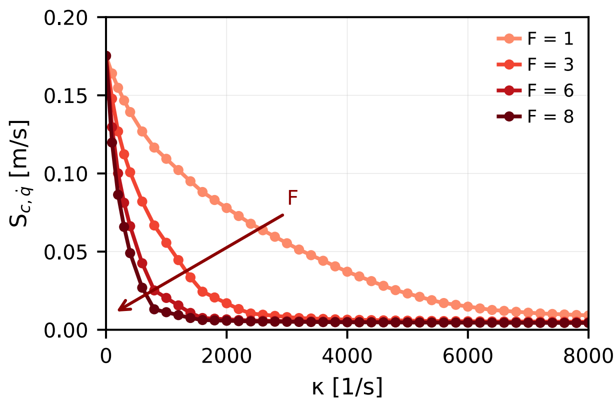

(a) Consumption speed plotted against κ

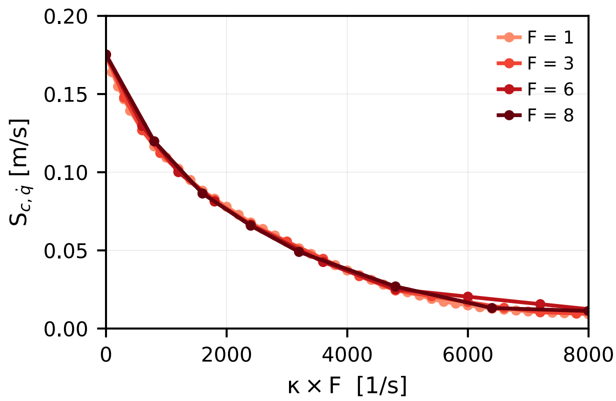

(b) Consumption speed plotted against $\kappa_{eff} = \kappa \times F$

Figure 2. Consumption speed $S_{c,\dot{q}}$ (as defined in Equation 4) of 1D methane-air ($\phi = 0.7$) RTP flames for various thickening factors

Impact of Thickening on a Global Chemical Kinetic Mechanism

Given that the artificially thickened flame model was first developed to be used with finite-rate chemistry models for LES [17], it is most common for a global chemical kinetic mechanism (1-3 reactions) to be used in LES due to the prohibitive computational cost of a detailed or in some cases skeletal mechanism. Hence one must consider how the consumption speed of a flame with a global chemical kinetic mechanism varies with thickening factor.

Franzelli et al.[18] showed that for lean CH_4-air flames, global mechanisms tend to over predict the consumption speed of a flame when stretched. Despite this general over prediction of consumption speed for lean CH_4-air flames, many authors have used global mechanisms in LES to predict flame shape and hence thermoacoustic results quite well[2,5,6].

To analyze this effect further, a 1D RTP flame is computed using a global mechanism for lean CH_4 combustion (that is also suited to low percentages of H_2) by Garcia et al.[7] named the 3S00H mechanism. The resulting consumption speed is plotted in Figure 3 for various thickening factors and for stretch levels of up to 8,000 (1/s). Also plotted is the consumption speed of the detailed C3MechLite mechanism with no thickening for comparison. It can be seen that the 3S00H, F=1 case over predicts the consumption speed of the detailed mechanism as expected. As the flame is thickened for the F=3,6,8 cases, it is seen that the consumption speed drops due to the flame experiencing a stretch level of $\kappa_{eff} = F \times \kappa$ as discussed in the previous subsection.

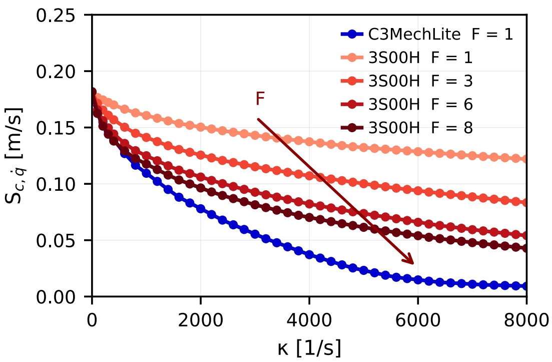

Figure 3. $S_{c,\dot{q}}$ vs κ for the 3S00H mechanism at $\phi = 0.7$

Hence, it can be concluded that as lean CH_4-air flames computed with a global mechanism are thickened, the consumption speed drops. It can be seen that the consumption speed of the 3S00H appears to get closer to the detailed mechanism with thickening factors of $F > 8$, but it should be noted that this does not imply that this is a thickening $F > 8$ should be used in a 3D LES simulation. Since the consumption speed in LES is a function of the efficiency function, thickening factor, flame stretch via straining and curvature, heat loss, and other hydrodynamic and thermochemical factors. This consumption speed will also vary along the flame. Furthermore, it is not expected that the scaling of the convective term with 1/F for 1D flames would apply in the same fashion to 3D turbulent flames, and hence there is likely a more complicated relationship between κ_{eff} and κ.

Nonetheless the trend holds that a global chemical kinetic mechanism for the case of lean CH_4 flames tends to overpredict $S_{c,\dot{q}}$, and this consumption speed tends to drop as the flame is thickened.

3D LES: NTNU Burner

LES was conducted using ANSYS Fluent 2023R2 on the NTNU bluff body combustor[19–21] due to its simple geometry and wealth of open source experimental data. The geometry is shown in Figure 4, where L_p = 145mm, L_g = 45mm,L_c = 80mm, d_g = 4mm. H is the flame length, which is calculated in the lean CH_4 case as being $H \approx 34$ mm.

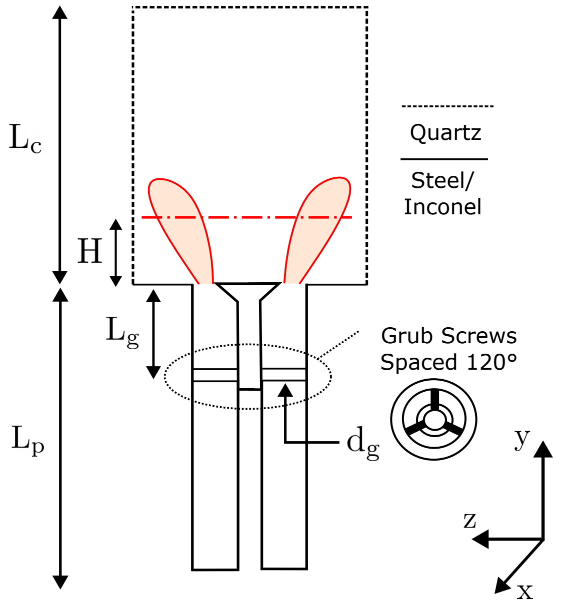

Figure 4. Experimental Setup with relevant length scales labeled (not to scale). Full experimental setup can be found in[20–22]

The CH_4-air case ($\phi = 0.7$) only is considered here. Conjugate heat transfer was applied to accurately represent flame dynamics[23], using the boundary conditions in Garcia et al.[7]. A structured, poly-hexcore mesh was created using Fluent Meshing resulting in 10.7M cells, with a cell size of $\Delta = 0.25$ mm at the flame and grub screws. The number of grid points in the flame is given by:

$$n = \frac{F\delta_L^0}{\Delta} \tag{5}$$

Simulations were performed with $n = 5, 7.5, 10$ which correspond to $F = 1.79, 2.69, 3.58$, given that the laminar flame thickness calculated from the 3S00H was given as $\delta_L^0 = 0.6986$ mm. The Charlette efficiency function is used in all cases, with a flame sensor based on reaction rate of CH_4 oxidation.

Shown in Figure 5 is the normalised heat release rate of each case, compared with the experimental OH* chemiluminescence. The experimental image is reconsructed using Abel Deconvolution. The effect of thickening on the mean flame shape can be clearly seen, where the increase in thickening resulted in a longer flame due to a drop in consumption speed. The outer shear layer also became less intense as the thickening factor increased. In a case with a further increase of thickening factor to $n = 15$ ($F = 5.37$), the outer shear layer extinguished and the flame transitioned from an M shaped flame to a V shaped flame (not shown here).

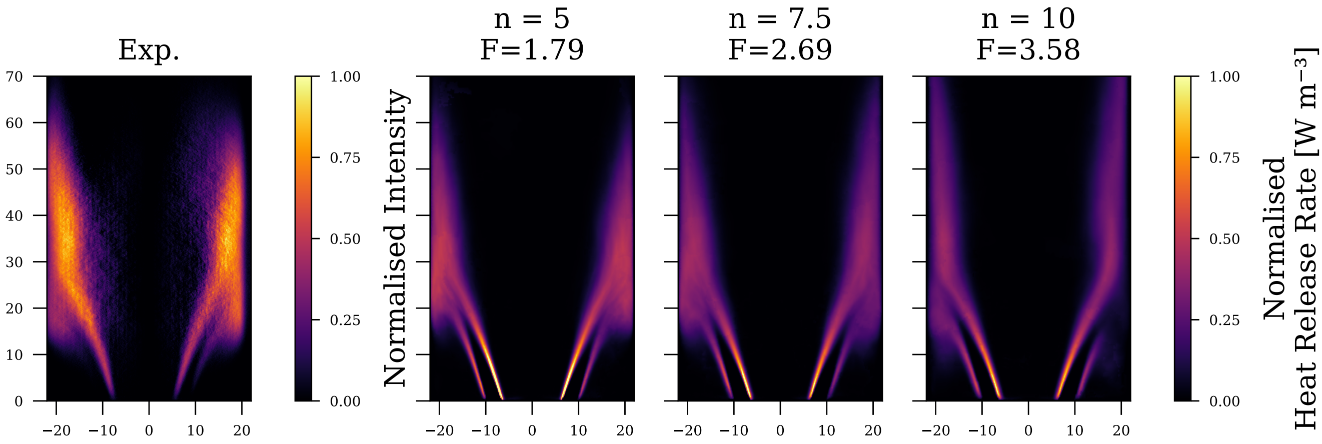

Figure 5. Comparison of normalised intensity of experimental OH* chemiluminescence to the normalised heat release rate from LES simulations with thickening factors $F = 1.79, 2.69, 3.58$. All dimensions in mm. Dashed lines show the flame length (centroid),H, for each case

To show the elongation of the flame with thickening more clearly, the integrated HRR in the axial direction is shown in Figure 6, where the area under each curve is normalized to be 7kW. The flame length (centroid height), H, is also shown using dashed lines for each case. It can be clearly seen that as F was increased, the flame length increased, and the extent of heat release increased along the length of the combustor. This is characteristic of a drop in consumption speed. It is also worth noting in the F=3.58 case the consumption speed dropped so much that the heat release rate at the outlet was non-zero. This indicates that the flame left the domain, and energy was not conserved. This has implications for determining the FTF which will be discussed in the next section.

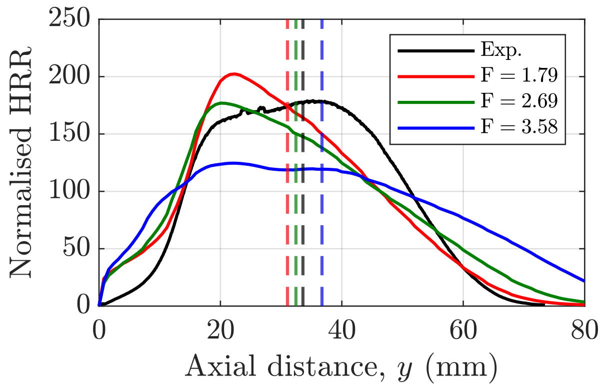

Figure 6. Comparison of integrated heat release rate (HRR) from LES simulations with $F = 1.79, 2.69, 3.58$ to the integrated experimental OH* chemiluminescence. Plotted against axial distance along the combustor. All plots normalised to have an area of 7kW.

Flame Transfer Function

The FTF of each case was computed using the LES System Identification (LES-SysID) methodology[24,25] for each case. This involved forcing the inlet velocity with a broadband signal, and extracting the velocity at the flame base (dump plane) and the volumetric heat release rate as the input and output respectively of a linear time invariant system. The auto correlation matrix, Γ, and the cross correlation vector, $\mathbf{c}$, were computed and used to calculate the impulse response (IR) vector $\mathbf{h}$ by inversion of the Weiner-Hopf equation:

$$\mathbf{h} = \Gamma^{-1}\mathbf{c} \tag{6}$$

More details can be found in[26,27]

Daubechies wavelet signals of length 0.2s with an amplitude of 6%, and frequency limited to 1000Hz, were generated using the TFD toolbox from Technical University of Munich[28,29]. The $F = 1.79, 2.69$ cases appeared sufficiently identified after 0.15s of data had been collected, to where changing the number of impulse response coefficents had minimal change on the FTF shape. The $F = 3.58$ case had a higher signal to noise ratio, and hence needed an LES run of 0.2s for reasonable identification of the FTF. The gain and phase of the FTF are shown in Figure 7.

Clear differences in the gain can be seen from each thickening factor. Firstly it can be seen that for the $F = 1.79$ case there were two modulations in the gain at $f \approx 270, 520$ Hz. The $F = 2.69$ case showed only one major peak in the gain at $f \approx 270$ Hz, and the $= 3.58$ showed no large peaks in the gain, and also showed no excess gain (i.e. $|\mathcal{F}(\omega)| > 1$). The $F = 2.69$ case appeared to have the closest match with the experimental gain, with a slight overprediction of excess gain at $f \approx 270$ Hz. The behavior of the phase was representative of the differences in flame length (as seen by the change in flame length for each case in Figure 6). There was minimal difference in the phase due to similar flame lengths, but a clear difference can be seen at higher frequencies (800-1000 Hz) where the phase of the $F = 1.79$ case had the largest slope, and this slope reduced as the flame was thickened, and hence the flame length increased.

Modulations in Gain

The LES-SysID workflow computes the impulse response (IR) vector $\mathbf{h}$, as computed using Equation 6. This impulse response vector can be used to analyze the key time delays that govern the dynamics of the system[30]. The IR for each

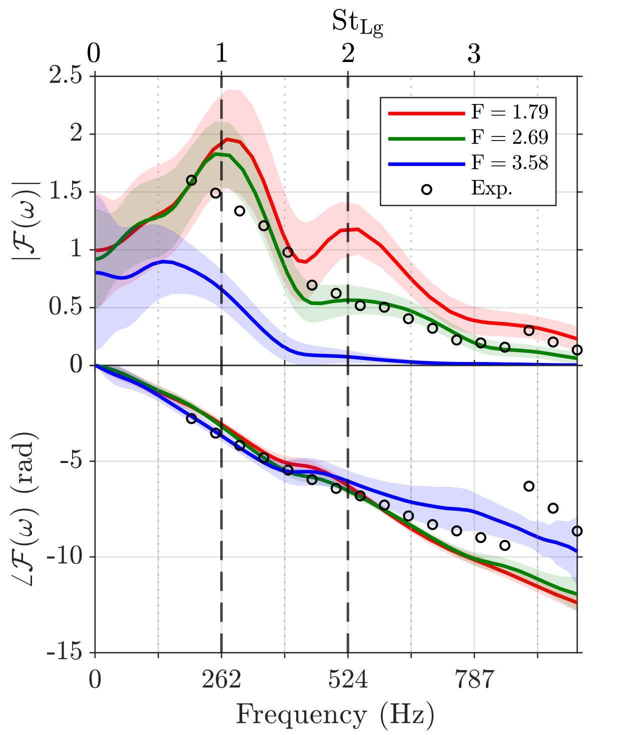

Figure 7. Flame Transfer Function of the $F = 1.79, 2.69, 3.58$ cases calculated using LES-SysID. Experimental values also shown. The top abscissa shows Strouhal number, calculated as per Equation 8, wheras the bottom abscissa shows frequency in Hz

case is shown in Figure 8. The first time delay captured by each case is $\tau_1 \approx \frac{\mathrm{H}}{\bar{u}_0}$ where H is the height of the flame and $\bar{u}_0$ is the mean velocity that exits the bluff body in the dump plane. This corresponds to the time delay from the flame base to the mean flame length. The second time delay corresponds to the delay from the grub screws to the mean flame height, $\tau_2 \approx \frac{\mathrm{L_g}}{\bar{u}_p} + \frac{\mathrm{H}}{\bar{u}_p}$, where L_g is the distance of the grub screws from the dump plane, and $\bar{u}_p$ is the average velocity in the inlet pipe. These length scales are shown in Figure 4.

It is clear from Figure 8 that the $F = 1.79$ and $F = 2.69$ cases interacted with these two time delays τ_1 and τ_2, wheras the $F = 3.58$ case only interacted with τ_1. The time delay τ_2 was shown experimentally to result in modulations in the gain and phase, and the physical mechanism is due to vortex shedding at the grub screws[22]. These modulations can occur when the flame length is small enough to result in a cut-off frequency that is less than or greater than the frequency of certain vortex shedding modes.

It was shown that if these grub screws are replaced with cylinders[31] (which is how the grub screws are modelled in LES) that the physical origin of the modulations are due to vortex shedding, which can be demonstrated using a Strouhal number scaling of:

$$\mathrm{St_{dg}} = \frac{f_s d_g}{\bar{u}_p} \tag{7}$$

where f_s is the shedding frequency, d_g is the diameter of the grub screws and $\bar{u}_p$ is the average velocity in the upstream pipe containing the grub screws.

There are various $\mathrm{St_{dg}}$ that the vortices can shed at[22], but it is noted that the largest experimental modulations were

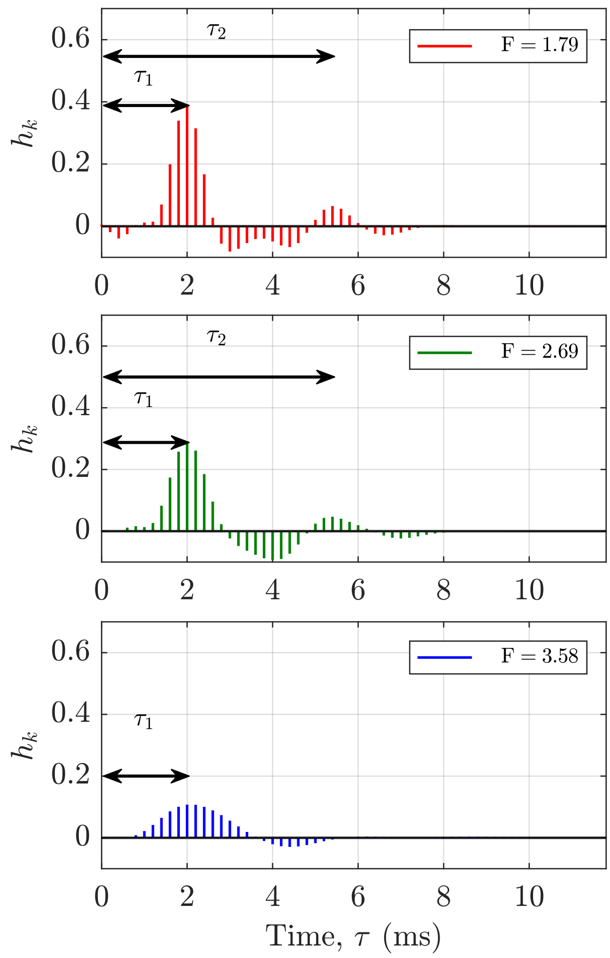

Figure 8. Impulse Response vector of each case $F = 1.79, 2.69, 3.58$, where the coefficients h_k of the unit impulse response vector **h** is plotted against time.

be seen in the range $\mathrm{St_{dg}} = 0.2 - 0.4$. While the physical origin of the vortex shedding is from the grub screws, the wavelength and hence characteristic time delay correspond best with the time delay $\tau_3 \approx \frac{L_g}{u_p}$ (where $\tau_3 = \tau_2 - \tau_1$)[31] which is the time taken for the vortex to reach the flame base. A Strouhal number based on this time lag is given as:

$$\mathrm{St_{Lg}} = \frac{f_s L_g}{u_p} = f_s \tau_3 \tag{8}$$

$\mathrm{St_{LG}}$ was plotted on the x axis in Figure 7, and it was seen that the modulations appeared at integers $\mathrm{St_{Lg}} \approx 1, 2$, corresponding to experimentally recorded values[31]. This corresponds to, for this case, $f_{s_1} \approx 262$ Hz and $f_{s_2} \approx 524$ Hz, which aligns with the modulations in gain.

The cut-off frequency of the flame, which identifies which vortex shedding modes can interact with the flame, can be estimated as the inverse of τ_1[32]:

$$f_c = \frac{1}{\tau_1} = \frac{\bar{u}_0}{H} \tag{9}$$

The cut-off frequency for each of thickening factor case, is shown in Table 1. Also plotted is the ratio of the first two vortex shedding modes f_{s_1} and f_{s_2} corresponding to $\mathrm{St_{Lg}} \approx 1, 2$ respectively. It was seen that as the thickening factor is increased from the $F = 1.79$ case to the $F = 3.58$ case, the cut-off frequency for the interaction with vortex modes decreased. It can be seen that once $f_{s_1}/f_c \approx 0.47$, the interact of this vortex shedding mode with the gain of the FTF became weak, as is evident from Figure 7. Furthermore, the $F = 1.79, 2.69$ cases both showed a modulation in the gain of the FTF at $\mathrm{St_{Lg}} = 1$ due to a lower value of f_{s1}/f_c. It is also evident in Figure 7 that the FTF gain only showed significant modulation at $\mathrm{St_{Lg}} = 2$ for the $F = 1.79$ case. This indicates that as f_{s_2}/f_c gets greater than approximately 0.79, the modulations of this mode to the FTF gain become negligible. It was also observed experimentally that vortex shedding modes can interact with the FTF gain at $\mathrm{St_{Lg}} = 3$ if the cut-off frequency allows.

Table 1. Flame heights, cut-off frequencies, and the ratios f_{s_1}/f_c and f_{s_2}/f_c for each case.

Case	H (mm)	f_c (Hz)	f_{s_1}/f_c	f_{s_2}/f_c
Exp.	33.6	610	0.43	0.86
$F = 1.79$	31.0	661	0.40	0.79
$F = 2.69$	32.4	633	0.41	0.83
$F = 3.58$	36.7	559	0.47	0.94

It is clear that changing thickening factors can cause the amplification or attenuation of modulations in the FTF gain. The main reason for these modulations changing is this case was shown to be due to changes in flame height and hence cut-off frequency at which shedding vortices can interact with the flame. It has been known that the ATF model can suppress flame wrinkling[33], which is accounted for by the efficiency function. Since flame wrinkling plays a very important role in determining the interaction of vortices with the flame in this case, future work will focus on computing the FTF using a coarser mesh, where the role of the efficiency function plays an important role in recovering flame wrinkling.

Low Frequency Gain Limit: Conservation of Energy

Another noticeable difference in the FTF's of each case was the low frequency gain limit, $|\mathcal{F}(\omega)|_{@f=0}$. Polifke and Lawn[34] showed that for a premixed flame, due to conservation of mass and energy considerations, this low frequency value should approach 1. As seen in Figure 7, as F increased, the low frequency gain limit decreased, indicating conservation laws for mass and/or energy were not conserved. A closer examination of the normalised HRR in Figure 6 shows that as the thickening factor increased the HRR at the outlet of the domain increased. The outlet is placed at $y = 80$ mm, and it was seen that for the $F = 1.79$ case, there was negligible HRR at the outlet. As F was increased to $F = 2.69$ it was seen that the HRR is slightly non zero at the outlet, and the $F = 3.58$ case showed a non negligible HRR at the outlet. This indicates that as the thickening factor was increased and the flame became longer, part of the flame started to leave the domain, and energy was no longer conserved. This is the reason for the reduction in low frequency gain limit with frequency, and also explains the large confidence interval in the FTF for the $F = 3.58$ case at the low frequency gain limit. Lengthening of the domain would increase the low frequency gain limit to 1 and allow for more accurate study of the dynamics of the flame at higher thickening factors, but it should be noted this is purely due to the numerics, and experimentally there is no evidence of non negligible HRR at the outlet.

A further increase of thickening factor $n = 15, F = 5.37$ showed a further decrease in the low frequency gain limit (and gain overall) due to the flame being too long to be resolved by the domain, and hence energy not being conserved.

Conclusion

This study explored the effect of flame thickening on the flame shape and dynamic response of a flame via the flame transfer function.

Firstly, a 1D reactant to product counter-flow flame was examined to analyze the impact of thickening on the consumption speed of a flame. This analysis was also extended to compare the behaviour of a global kinetic mechanism, which is suited for Large Eddy Simulations (LES), with that of a detailed kinetic mechanism.

Full 3D LES was then conducted on a lean CH_4-air combustor test case with three thickening factors, $F = 1.79, 2.69$ and $F = 3.58$ corresponding to differing numbers of cells across the flame front $n = 5, 7.5, 10$ respectively. The trends shown from the 1D flames were also examined in the 3D LES, where thickening of the flame tends to reduce the consumption speed of a lean CH_4-air flame. This manifested itself as a reduction in flame length, and a heat release rate which was distributed over a larger length.

The Flame Transfer Function (FTF) was then computed using the system identification workflow. There was a decrease in phase at larger frequencies as thickening factor was increased. A more noticible difference was shown in the gain of each case. The $F = 1.79$ case showed peaks in the gain at $f \approx 270, 520$Hz, wheras the $F = 2.69$ case only showed the peak at $f \approx 270$ Hz, and the $F = 3.58$ case showed no peaks in gain. These peaks in the gain were shown to correspond to vortex shedding modes from the cylinder, with wavelengths corresponding to a Strouhal number based on the distance of upstream cylinders to the base of the flame.

It should be noted that the FTF obtained using a thickening factor of $F = 2.69$ represented the gain and phase of the experiment reasonably well, wheras the FTF's obtained using thickening factors of $F = 1.79$ and $F = 3.58$ showed clear and distinct differences, mainly in the gain.

It was shown that the $F = 3.58$ case had an unphysical low frequency limit in the FTF gain due to lack of conservation of energy. This was due to the flame leaving the domain of the combustor, as a result of the drop in consumption speed induced by the thickening factor.

This paper clearly highlights the how the thickening factor used in the Artifically Thickened Flame model can impact the flame transfer function, and likewise the impulse response.

References

1. Lieuwen TC and Yang V. *Combustion Instabilities in Gas Turbine Engines: Operational Experience, Fundamental Mechanisms and Modeling*. American Institute of Aeronautics

and Astronautics, 2005. ISBN 978-1-56347-669-3. Google-Books-ID: 4_pTAAAAMAAJ.

2. Franzelli B, Riber E, Gicquel LYM et al. Large Eddy Simulation of combustion instabilities in a lean partially premixed swirled flame. *Combustion and Flame* 2012; 159(2): 621–637. DOI:10.1016/j.combustflame.2011.08.004. URL https://www.sciencedirect.com/science/article/pii/S0010218011002525.
3. Kraus C, Selle L and Poinsot T. Coupling heat transfer and large eddy simulation for combustion instability prediction in a swirl burner. *Combustion and Flame* 2018; 191: 239–251. DOI:10.1016/j.combustflame.2018.01.007. URL https://www.sciencedirect.com/science/article/pii/S0010218018300117.
4. Staffelbach G, Gicquel LYM, Boudier G et al. Large Eddy Simulation of self excited azimuthal modes in annular combustors. *Proceedings of the Combustion Institute* 2009; 32(2): 2909–2916. DOI:10.1016/j.proci.2008.05.033. URL https://www.sciencedirect.com/science/article/pii/S154074890800093X.
5. Eder AJ, Silva CF, Haeringer M et al. Incompressible versus compressible large eddy simulation for the identification of premixed flame dynamics. *International Journal of Spray and Combustion Dynamics* 2023; 15(1): 16–32. DOI:10.1177/17568277231154204. URL https://doi.org/10.1177/17568277231154204.
6. Désor M, Haeringer M, Hiestermann M et al. Application of an Improved Workflow for the Identification of Flame Dynamics to Swirl-Stabilized Wet Combustion. *Journal of Engineering for Gas Turbines and Power* 2024; 147(031003). DOI:10.1115/1.4066364. URL https://doi.org/10.1115/1.4066364.
7. Garcia AM, Le Bras S, Prager J et al. Large eddy simulation of the dynamics of lean premixed flames using global reaction mechanisms calibrated for CH4–H2 fuel blends. *Physics of Fluids* 2022; 34(9): 095105. DOI:10.1063/5.0098898. URL https://doi.org/10.1063/5.0098898.
8. Kuhlmann J, Lampmann A, Pfitzner M et al. Assessing accuracy, reliability, and efficiency of combustion models for prediction of flame dynamics with large eddy simulation. *Physics of Fluids* 2022; 34(9): 095117. DOI:10.1063/5.0098975. URL https://doi.org/10.1063/5.0098975.
9. Popp S, Kuenne G, Janicka J et al. An extended artificial thickening approach for strained premixed flames. *Combustion and Flame* 2019; 206: 252–265. DOI:10.1016/j.combustflame.2019.04.047. URL https://www.sciencedirect.com/science/article/pii/S0010218019301981.
10. Detomaso N, Hok JJ, Dounia O et al. A generalization of the Thickened Flame model for stretched flames. *Combustion and Flame* 2023; 258: 113080. DOI:10.1016/j.combustflame.2023.113080. URL https://www.sciencedirect.com/science/article/pii/S0010218023004558.
11. Rathore O and Navarro-Martinez S. Flame Dynamics Modelling Using Artificially Thickened Models. *Flow, Turbulence and Combustion* 2023; 111(3): 897–927. DOI:10.1007/s10494-023-00433-2. URL https://doi.org/10.1007/s10494-023-00433-2.
12. Poncet S, Mehl C, Truffin K et al. A Thickened Flame Model adaptation to weakly stretched flames for non-unity Lewis number mixtures. *Combustion and Flame* 2024; 270: 113758. DOI:10.1016/j.combustflame.2024.113758. URL https://www.sciencedirect.com/science/article/pii/S001021802400467X.
13. Goodwin D, Moffat H and Speth R. *Cantera: An Object-oriented Software Toolkit for Chemical Kinetics, Thermodynamics, and Transport Processes. Version 2.2.0*. 2015. DOI:10.5281/zenodo.48735.
14. Garcia AM, Bras SL and Polifke W. Effect of hydrogen addition on the consumption speed of lean premixed laminar methane flames exposed to combined strain and heat loss. *Combustion Theory and Modelling* 2023; 27(4): 584–604. DOI:10.1080/13647830.2023.2182235. URL http://arxiv.org/abs/2211.15171. ArXiv:2211.15171 [physics].
15. CERFACS. Cantera-avbp. https://gitlab.com/cerfacs/chemistry/cantera-avbp, 2025. Accessed: 2025-05-14.
16. Dong S, Wagnon SW, Pratali Maffei L et al. A new detailed kinetic model for surrogate fuels: C3MechV3.3. *Applications in Energy and Combustion Science* 2022; 9: 100043. DOI:10.1016/j.jaecs.2021.100043. URL https://www.sciencedirect.com/science/article/pii/S2666352X21000212.
17. Colin O, Ducros F, Veynante D et al. A thickened flame model for large eddy simulations of turbulent premixed combustion. *Physics of Fluids* 2000; 12(7): 1843–1863. DOI:10.1063/1.870436. URL https://doi.org/10.1063/1.870436.
18. Franzelli B, Riber E and Cuenot B. Impact of the chemical description on a Large Eddy Simulation of a lean partially premixed swirled flame. *Comptes Rendus Mécanique* 2013; 341(1): 247–256. DOI:10.1016/j.crme.2012.11.007. URL https://www.sciencedirect.com/science/article/pii/S163107211200215X.
19. Æsøy E. *The Effect of Hydrogen Enrichment on the Thermoacoustic Behaviour of Lean Premixed Flames*. Doctoral thesis, NTNU, 2022. URL https://ntnuopen.ntnu.no/ntnu-xmlui/handle/11250/2838552.
20. Æsøy E, Aguilar J, Wiseman S et al. Scaling and Prediction of Transfer Functions in Lean Premixed H2 /CH4 -Flames. *Combustion and Flame* 2020; 215: 269–282. DOI:10.1016/j.combustflame.2020.01.045.
21. Aguilar JG, Æsøy E and Dawson JR. The influence of hydrogen on the stability of a perfectly premixed combustor. *Combustion and Flame* 2022; 245: 112323. DOI:10.1016/j.combustflame.2022.112323. URL https://www.sciencedirect.com/science/article/pii/S0010218022003388.
22. Æsøy E, Aguilar JG, Bothien MR et al. Acoustic-Convective Interference in Transfer Functions of Methane/Hydrogen and Pure Hydrogen Flames. *Journal of Engineering for Gas Turbines and Power* 2021; 143(121017). DOI:10.1115/1.4051960. URL https://doi.org/10.1115/1.4051960.
23. Agostinelli PW, Laera D, Boxx I et al. Impact of wall heat transfer in Large Eddy Simulation of flame dynamics in a swirled combustion chamber. *Combustion and Flame* 2021; 234: 111728. DOI:10.1016/j.combustflame.2021.111728. URL https://www.sciencedirect.com/science/article/pii/S0010218021004715.

24. Huber A and Polifke W. Dynamics of Practical Premixed Flames, Part I: Model Structure and Identification. *International Journal of Spray and Combustion Dynamics* 2009; 1(2): 199–228. DOI:10.1260/175682709788707431. URL https://doi.org/10.1260/175682709788707431.
25. Huber A and Polifke W. Dynamics of Practical Premixed Flames, Part II: Identification and Interpretation of CFD Data. *International Journal of Spray and Combustion Dynamics* 2009; 1(2): 229–249. DOI:10.1260/175682709788707440. URL https://doi.org/10.1260/175682709788707440.
26. Polifke W. Black-box system identification for reduced order model construction. *Annals of Nuclear Energy* 2014; 67: 109–128. DOI:10.1016/j.anucene.2013.10.037. URL https://www.sciencedirect.com/science/article/pii/S0306454913005768.
27. Polifke W. System identification for aero- and thermo-acoustic applications. Lecture notes presented at the Lecture Series "Advances in Aero- and Thermo-Acoustics", 2010. Corrected printing: 9 May 2011. Technische Universität München.
28. Polifke W, Eder AJ and Desor M. TFD tools. *Private Communication* 2024; .
29. Föller S and Polifke W. Advances in Identification Techniques for Aero-Acoustic Scattering Coefficients from Large Eddy Simulation. In *18th International Congress on Sound and Vibration*, volume 4. Rio de Janeiro, Brazil: International Institute of Acoustics & Vibration. ISBN 978-1-61839-259-6, pp. 3122–3129.
30. Komarek T and Polifke W. Impact of Swirl Fluctuations on the Flame Response of a Perfectly Premixed Swirl Burner. *Journal of Engineering for Gas Turbines and Power* 2010; 132(061503). DOI:10.1115/1.4000127. URL https://doi.org/10.1115/1.4000127.
31. Æsøy E, Nygård HT, Worth NA et al. Tailoring the gain and phase of the flame transfer function through targeted convective-acoustic interference. *Combustion and Flame* 2022; 236: 111813. DOI:10.1016/j.combustflame.2021.111813. URL https://www.sciencedirect.com/science/article/pii/S0010218021005563.
32. Kutkan H. Modelling Turbulent Premixed CH4/H2/air Flames with Effects of Stretch, Heat Loss and Non-unity Lewis Number for Flame Stabilization and Dynamics 2023; DOI:10.15167/kutkan-halit_phd2023-05-23. URL https://iris.unige.it/handle/11567/1117856. Accepted: 2023-05-11T08:37:17Z Publisher: Università degli studi di Genova.
33. Poinsot T and Veynante D. *Theoretical and Numerical Combustion*. Edwards, 2001.
34. Polifke W and Lawn C. On the low-frequency limit of flame transfer functions. *Combustion and Flame* 2007; 151(3): 437–451. DOI:10.1016/j.combustflame.2007.07.005. URL https://www.sciencedirect.com/science/article/pii/S0010218007001952.